



RESEARCH ARTICLE

10.1029/2019GC008734

Key Points:

- We estimate the range of $p\text{CO}_2$, surface temperature, and ocean pH in the Hadean and Archean
- A cold, Hadean surface environment and circumneutral to basic ocean pH is likely because of impact ejecta weathering
- The origin of life may have occurred in a cold environment, and early life may have spread into a cold alkaline ocean

Supporting Information:

- Supporting Information S1

Correspondence to:

S. Kadoya,
skadoya@uw.edu

Citation:

Kadoya, S., Krissansen-Totton, J., & Catling, D. (2020). Probable cold and alkaline surface environment of the Hadean Earth caused by impact ejecta weathering. *Geochemistry, Geophysics, Geosystems*, 21, e2019GC008734. <https://doi.org/10.1029/2019GC008734>

Received 27 SEP 2019

Accepted 19 DEC 2019

Accepted article online 22 DEC 2019

Probable Cold and Alkaline Surface Environment of the Hadean Earth Caused by Impact Ejecta Weathering

Shintaro Kadoya¹, Joshua Krissansen-Totton², and David C. Catling¹

¹Department of Earth and Space Sciences, Cross-Campus Astrobiology Program, University of Washington, Seattle, WA, United States, ²Department of Astronomy and Astrophysics, University of California, Santa Cruz, CA, United States

Abstract Constraining the surface environment of the early Earth is essential for understanding the origin and evolution of life. The release of cations from silicate weathering depends on climatic temperature and $p\text{CO}_2$, and such cations sequester CO_2 into carbonate minerals in or on the seafloor, providing a stabilizing feedback on climate. Previous studies have suggested that this carbonate-silicate cycle can keep the early Earth's surface temperature moderate by increasing $p\text{CO}_2$ to compensate for the faint young Sun. However, the Hadean Earth experienced a high meteorite impactor flux, which produced ejecta that is easily weathered by carbonic acid. In this study, we estimated the histories of surface temperature and ocean pH during the Hadean and early Archean using a new model that includes the weathering of impact ejecta, empirically justified seafloor weathering, and ocean carbonate chemistry. We find that relatively low $p\text{CO}_2$ and surface temperatures are probable during the Hadean, for example, at 4.3 Ga, $\log_{10}(p\text{CO}_2)$ (in bar) is $-2.21^{+3.01}_{-2.54}$ [2σ] and temperature is $259.2^{+84.1}_{-14.4}$ [2σ] K. Such a low $p\text{CO}_2$ would result in a circumneutral to basic pH of seawater, for example, $7.90^{+1.21}_{-1.69}$ [2σ] at 4.3 Ga. A probably cold and alkaline marine environment is associated with a high impact flux. Hence, if there was an interval of an enhanced impact flux, that is, Late Heavy Bombardment, similar conditions may have existed in the early Archean. Therefore, if the origin of life occurred in the Hadean, life likely emerged in a cold global environment and probably spread into an alkaline ocean.

Plain Language Summary The Earth's environment during the Hadean eon, 4.5 to 4 billion years ago, is obscured by a lack of geological evidence. However, life likely arose then, so improving our knowledge of the early environment is essential for understanding the origin and evolution of life. Here, we build a geological carbon cycle model that simulates the early surface environment and generates probability distributions for the level of atmospheric carbon dioxide (CO_2), average surface temperature, and ocean pH over time. During the Hadean, CO_2 dissolved in water is consumed by reacting with material ejected from meteorite impacts, so CO_2 levels tend to be low and the greenhouse effect weak. The consequences are low surface temperature and alkaline seawater. The probability that the surface temperature was lower than the freezing point of water and that seawater pH exceeded 7 is 70% at 4.3 billion years ago. Thus, if life began in the Hadean, it likely emerged in a cold global environment, and early life may have spread into an alkaline ocean.

1. Introduction

Life arose on the Earth probably after the last ocean-vaporizing impact between 4.5 to 4.2 Ga (Marchi et al., 2014) but before possible signs of life at 3.5 to 3.8 Ga (e.g., Knoll & Nowak, 2017). Low $^{13}\text{C}/^{12}\text{C}$ of graphitic inclusions within a Hadean zircon may indicate the existence of biosphere as early as 4.1 Ga (Bell et al., 2015). However, exactly how and where life arose is unknown. Subsequently, life populated the ancient ocean as shown by a global modulation of carbon isotopes of marine carbonates and organic matter, dating from at least 3.5 Ga (Buick, 2001). Hence, it is essential to constrain the early environment to make progress on our understanding of the origin of life and the subsequent survival and dispersal of life. However, it is difficult to determine environmental constraints during the Hadean eon (~4.5 to 4 Ga), because geological evidence is limited.

Some inferences about the Hadean have been made from zircon geochemistry. Oxygen isotopes from zircons indicate the existence of an ocean after 4.2 Ga (e.g., Wilde et al., 2001; Valley et al., 2002), while studies of strontium isotopes suggest the presence of felsic continental crust by 4.4–4.2 Ga (Boehnke et al., 2018).

©2019. The Authors.

This is an open access article under the terms of the Creative Commons Attribution License, which permits use, distribution and reproduction in any medium, provided the original work is properly cited.

Some phylogenetic analyses have been used to argue for thermophilic ancestors and a hot ocean on the early Earth (e.g., Gaucher et al., 2008), but other studies (e.g., Boussau et al., 2008; Cantine & Fournier, 2018; Catchpole & Forterre, 2019) convincingly suggest a mesophilic Last Universal Common Ancestor, that is, with optimum growth temperature of $<50^{\circ}\text{C}$. Indeed, deeply rooted thermophiles on the tree of life may just be an artifact because other microbial lineages were wiped out by large meteorite impacts in the Hadean, while subsurface thermophiles survived (e.g., Nisbet & Sleep, 2001; Sleep et al., 1989).

Evidence and models suggest that the surface environment of the Earth is controlled by the carbonate-silicate cycle on timescales of $\sim 10^6$ years (e.g., Berner & Kothavala, 2001; Franck et al., 2002; Krissansen-Totton & Catling, 2017; Walker et al., 1981). As shown in previous papers (e.g., Charnay et al., 2017; Krissansen-Totton et al., 2018), the negative feedback of the cycle has maintained moderate surface temperatures at least since the Archean. Indeed, the negative feedback has decreased atmospheric CO_2 over geologic time driven by an increasingly brighter Sun. In addition, the long-term decrease in the atmospheric CO_2 allowed ocean pH to increase over time. Hence, the implications of the carbonate-silicate cycle are that the Archean Earth had a moderate surface temperature and a less alkaline ocean relative to today.

Reverse weathering is a possible modulation of the carbonate-silicate cycle in which cations are precipitated in clay minerals rather than in carbonates (that take up carbon), allowing CO_2 to remain in the atmosphere. In particular, it has been proposed that Precambrian reverse weathering could have been more important than on the modern Earth because the lack of biosilicification resulted in a high concentration of marine dissolved silica (DSi) that enhanced clay formation (Isson & Planavsky, 2018). However, during the Hadean and the early Archean, the concentration of DSi should be low since the influx of DSi to the ocean and sedimentation rates were low because of the likely smaller land mass (Bada & Korenaga, 2018). Thus, reverse weathering was probably unimportant during Hadean, which is the focus of this paper. Consequently, we did not include reverse weathering in this study. However, the impact of the reverse weathering on the climate of the early Earth will be the subject of the future study.

A moderation of the Hadean climate by the carbonate-silicate cycle similar to that in the Archean might be expected, but a high flux of meteorite impacts must be taken into account. Although the immediate aftermath of impacts can produce hot climates, the effect would only be transient. For example, the hot environment from impactors comparable in size to those that produced the Orientale, Imbrium, and South Pole-Aitken craters on the Moon would last only ~ 100 year (e.g., Nisbet et al., 2007).

On geological timescales of 10^6 years or more, comparable to that on which the carbonate-silicate cycle operates, the overall effect of impacts in the Hadean would be to cool the Earth. Impacts produce considerable ejecta, which is easily weathered by carbonic acid (Charnay et al., 2017; Sleep & Zahnle, 2001; Zahnle & Sleep, 2002). Such acid weathering of the impact ejecta is a source of carbonate alkalinity (i.e., dissolved cations), so it results in a decrease in atmospheric CO_2 when those cations sequester carbon into carbonates. Hence, the surface environment could be cool or even cold (i.e., snowball Earth) during the Hadean on the $\sim \text{Myr}$ timescale of the carbonate-silicate cycle, which is far longer than that of the transient impact heating discussed above (Charnay et al., 2017; Sleep & Zahnle, 2001; Zahnle & Sleep, 2002).

Moreover, the supply of carbonate alkalinity via ejecta weathering and/or more intense volcanic activity should result in an increase in seawater pH (Kempe & Degens, 1985; Sleep & Zahnle, 2001; Zahnle & Sleep, 2002). However, such an increase in pH was not included in the models of previous studies (Charnay et al., 2017; Sleep & Zahnle, 2001; Zahnle & Sleep, 2002). Seawater pH is potentially important because seafloor weathering is both pH and temperature dependent (Krissansen-Totton & Catling, 2017). Also, seafloor weathering likely helped buffer the surface temperature of the Archean Earth and is particularly important if continental weathering on the early Earth was diminished by a lack of land (Krissansen-Totton et al., 2018).

In this study, we estimated the evolution of surface environment on the early Earth based on our new carbonate-silicate cycle model. The model incorporates the estimated change of the impactor flux through time, impact ejecta weathering, continental weathering, seafloor weathering, and ocean carbonate chemistry and pH.

2. Model

2.1. Overview of Model

The model used in this study is essentially the same as that of Krissansen-Totton et al. (2018) except that we also include ejecta weathering. Here, we briefly describe the model, especially the model of ejecta weathering. For more detail, see Krissansen-Totton et al. (2018) and its references in addition to the supporting information of this study.

We estimate changes in the surface environment of the Earth through time based on the evolution of carbonate alkalinity and dissolved inorganic carbon of the ocean and seafloor pore space. Their evolution can be written as follows:

$$\begin{cases} Mo \frac{dA_o}{dt} = -J(A_o - A_p) + 2(F_{sil} + F_{carb} + F_{ej} - F_{pre, o}) \\ Mo \frac{dC_o}{dt} = -J(C_o - C_p) + F_{out} + F_{carb} - F_{pre, o} \\ Mp \frac{dA_p}{dt} = J(A_p - A_o) + 2(F_{diss} - F_{pre, p}) \\ Mp \frac{dC_p}{dt} = J(C_p - C_o) - F_{pre, p} \end{cases}, \quad (1)$$

where t is time ([Gyr]) and the subscripts o and p represent ocean and seafloor pore space, respectively. The parameter, A , represents the carbonate alkalinity. The parameter, C_o , represents the sum of the dissolved inorganic carbon in the ocean and the atmospheric CO_2 , and the parameter, C_p , represents the dissolved inorganic carbon in the pore space. Both A and C are in units of [mol/kg]. Fluxes in these equations, in units of [TmolC/yr], are volcanic CO_2 degassing (F_{out}), silicate weathering (F_{sil}), carbonate weathering (F_{carb}), seafloor weathering (F_{diss}), ejecta weathering (F_{ej}), and precipitation (F_{pre}). Here, J represents the mixing rate between the ocean and pore space in units of [10^{12} kg/year]. The ocean mass, Mo , is $1.35e21$ [kg], and the pore-space mass, Mp , is assumed to be 1% of Mo .

For simplicity, we neglect evolution of the carbon reservoirs of the mantle, and oceanic and continental crusts. In addition, we treat degassing from the mid-ocean ridge and from arc volcanoes as a single parameter, F_{out} . These assumptions do not meaningfully affect the results (Krissansen-Totton et al., 2018).

We randomly sample unknown parameters within each parameter range. The randomly sampled parameters and their parameter ranges are summarized in Tables S1 and S2 (for further information, see Krissansen-Totton et al., 2018, and references therein).

We assumed that the parameters are independent from each other and uniformly distributed within each parameter range to obtain a very conservative range of evolution, such as of pCO_2 and of surface temperature. Some parameters (e.g., sedimentary thickness on oceanic crust in equation (S15)) might depend on other parameters (e.g., seafloor spreading rate), and applying such a relation might limit the evolutionary range. However, the relationships are unknown and disputed, especially for the Hadean, so choosing a specific relationship among many in the literature might cause us to underestimate the evolutionary range. Instead, we err on the side of caution. In addition, since the parameter ranges are set by coupling independent estimates (Krissansen-Totton et al., 2018), the probability distribution of each parameter is uncertain. Thus, to avoid underestimation rather than overestimation of the range, we employ the above conservative assumptions.

2.2. Ejecta Weathering

The ejecta weathering depends on the amount and size distribution of the ejecta particles (e.g., Charnay et al., 2017; Sleep & Zahnle, 2001). The amount of the ejecta, m_{ej} , can be calculated as follows:

$$\frac{dm_{ej}}{dt} = p_{ej} - \frac{1}{c_{ej}} F_{ej} - r_{sub}, \quad (2)$$

where p_{ej} is the ejecta production rate and r_{sub} is the ejecta loss rate caused by resurfacing of the Earth and loss to the mantle due to subduction or the geological process that preceded subduction (Sleep, 2015). The coefficient, c_{ej} , represents the cation content in a ejecta particle, which is 5 mol/kg (Zahnle & Sleep, 2002).

For p_{ej} , we assume the same model as that of Charnay et al. (2017), which is based on the results of Collins et al. (2005). In this model, the amount of ejecta can be calculated using mass, velocity, density, and impact

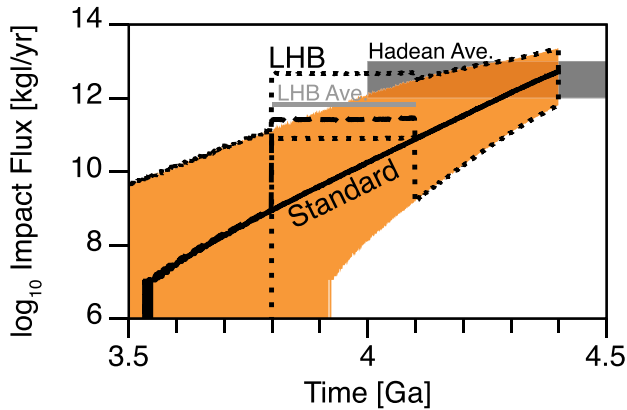


Figure 1. Modeled impact flux as a function of time. Solid black line and orange shaded region represent the median value and 95% confident interval for the standard evolution, respectively. On the other hand, black dashed and dotted lines represent the median value and 95% confident interval for the case with late heavy bombardment (LHB), respectively. The gray shaded region represents the average impact flux during the Hadean (Sleep & Zahnle, 2001). The horizontal gray solid line represents the average impact flux during the LHB (Charnay et al., 2017).

angle of each impact (see equations (S21) and (S22)). We assumed asteroid impacts, as in Charnay et al. (2017), that is, with a typical velocity of 21 km/s, density of $3\text{e}3 \text{ kg/cm}^3$, and typical impact angle of 45° .

We assumed an impact frequency as a function of impactor mass given by Anbar et al. (2001) and Sleep and Zahnle (2001):

$$f_{imp}(\geq m_{imp}) = f_{imp,0}(t) \times \left(\frac{m_{imp}}{m_{imp,max}} \right)^{-b_{imp}}, \quad (3)$$

where f_{imp} is an impact frequency having a mass equal to or higher than m_{imp} . Following Charnay et al. (2017), we assumed that the maximum mass of the impactor, $m_{imp,max}$, is 10^{19} kg , which is several times of the impactor mass of Imbrium and Orientale. The exponent, b_{imp} , is estimated to be between $2/3$ and $5/6$ (Anbar et al., 2001; Sleep & Zahnle, 2001).

We assumed that the coefficient, $f_{imp,0}$, in equation (3) decreases exponentially with time:

$$f_{imp,0} = f_{imp,ref} \times \exp \left\{ -\frac{t}{tdc} \right\}. \quad (4)$$

Based on Sleep et al. (1989) and Neukum et al. (2001), the decay timescale of the impact flux, tdc , is between 0.06 and 0.14 Gyr.

Sleep and Zahnle (2001) estimated that the Earth was hit by $5 \times 10^{20} \text{ kg}$ of material for initial 0.5 Gyr based on the lunar crater and considering the difference in cross-sectional area of the Earth and the Moon. Hence, we used a value of $f_{imp,ref}$ that reproduces the average impact flux between 10^{12} and 10^{13} kg/year for a given value of tdc . For comparison, highly siderophile element (HSE) in the mantle implies that assuming chondritic composition, $7 \times 10^{21} \text{ kg}$ to $3 \times 10^{22} \text{ kg}$ of impactors accreted to the Earth after the core formation (i.e., the late veneer) (Sleep, 2016, and the references therein). Thus, the Earth might experience more massive meteorite impact than we assumed. However, it is also suggested that such HSE is supplied to the Earth mainly by the Theia (i.e., the Moon-forming impactor) (e.g., Sleep, 2016) or by a single Moon-sized impactor (e.g., Genda et al., 2017). In such cases, most of the impactor mass corresponding to the late veneer was concentrated in the large impactors. Thus, the impact flux at the late Hadean, during which life might arise, should be lower than the total impactor mass of the late veneer (i.e., $\sim 10^{22} \text{ kg}$). To investigate the effect of meteorite impact conservatively, we retain the relatively low estimate.

Also, we calculated the impact flux assuming that the impact follows a Poisson distribution whose number of occurrence is calculated by equation (3). The modeled history of impact flux is shown in Figure 1 as a standard evolution of impact flux.

The ejecta weathering rate depends on the size distribution of ejecta particles. According to Collins et al. (2005), we assumed the initial size distribution of ejecta particles as follows:

$$N(\geq m_{ej}) = N0 \left(\frac{m}{m_{ej,max}} \right)^{-\gamma_{imp}}, \quad (5)$$

where N is a cumulative number of ejecta particles whose mass is larger than m_{ej} . The coefficient, γ_{imp} , is assumed to be between 0.87 and 0.95 (Charnay et al., 2017; Collins et al., 2005; Zahnle & Sleep, 2002). The coefficient, $N0$, is chosen so that it reproduces the total ejecta mass (see equation (A.20) in the supporting information). And we assumed that the radius of the largest ejecta is 100 m according to Charnay et al. (2017) and set the reference mass, $m_{ej,max}$, at $1.3 \times 10^{10} \text{ kg}$.

We assumed that the ejecta weathering occurs at the surface of ejecta particles; therefore, the radial shrinkage rate of ejecta does not depend on the radius itself. According to Gislason and Oelkers (2003), the shrink rate (v_{ej}) depends on temperature (T) and mole fraction of hydrogen ions ($[H^+]$) in aqueous solution, as follows:

$$ve_j = ve_{j,0} \exp \left\{ -\frac{25[\text{kJ}]}{RT} \right\} [\text{H}^+], \quad (6)$$

where R is the molar gas constant. The coefficient, $ve_{j,0}$ is calculated so that ve_j is 3 mm/Myr at $\text{pH} = 8$ and 60°C , which matches experimental data (Crovisier et al., 1987).

2.3. Seafloor and Ejecta Weathering in the High pH Limit

Considering the range of carbonate alkalinity (Krissansen-Totton et al., 2018), oceanic crust and impact ejecta reach a state of thermodynamic equilibrium if the pH of surrounding water is around 8–10. In other words, if the pH is higher than these values, weathering of the seafloor and/or ejecta weatherings stops because of oversaturation. In this study, we assumed that seafloor and ejecta weathering decrease if pH is higher than a certain threshold. For a standard calculation, we set the nominal threshold pH at 9 based on thermodynamic calculations. For these calculations, we used thermodynamic properties given by Johnson et al. (1992) and Zimmer et al. (2016). Detail information on the threshold can be seen in section S1.6. However, we also did sensitivity tests for this threshold pH to show that the exact value does not affect our overall conclusions (section S3.1).

3. Results

A typical model run shows a history with a cold climate and associated low ($p\text{CO}_2$) in the early Hadean when the impact flux was high. Figure 2 shows such results when we use the standard evolution of impact flux shown in Figure 1 and all the model parameters in Tables S1 and S2 are set at values summarized in Table S7. In Figure 2, we see (a) the imposed impact history and the modeled evolution of (b) partial pressure of atmospheric CO_2 ($p\text{CO}_2$) and (c) surface temperature.

Considering the case without ejecta weathering (hereafter, the “control” case), $p\text{CO}_2$ is higher at 4.4 Ga than 3.5 Ga (Figure 2b). The increase of $p\text{CO}_2$ backward in time results from a decrease of luminosity and an increase of CO_2 degassing rate that overwhelms any increase in seafloor weathering from increased seafloor spreading. Consequently, the surface temperature of the control case is higher at 4.4 Ga than at 3.5 Ga (Figure 2b).

Between 4.4 and 4.3 Ga, $p\text{CO}_2$ and the surface temperature of the case with ejecta weathering (hereafter, the “standard” case) are much lower than those of the control case as shown in Figures 2b and 2c. This is because of the high impact flux during this time period (Figure 2a), which results in the large production of ejecta that consumes CO_2 . Since the amount of the impactors that hit the Earth generally decreased with time (Figure 2a), the production of impact ejecta also decreased with time. Hence, the $p\text{CO}_2$ and surface temperature of the standard case increase and become gradually closer to that of the control case (Figures 2b and 2c). However, occasional large impacts still result in the lowering of $p\text{CO}_2$ and surface temperature. For example, in this calculation, large impacts corresponding to the Imbrium impactor (e.g., 2×10^{18} kg; Baldwin, 1987) occur around 4.1 Ga (Figure 2a). These impacts result in negative excursions of $p\text{CO}_2$ and surface temperature (Figures 2b and 2c).

Figure 3 shows the evolution of surface environment that is based on the calculations of 10,000 different parameter sets, where each parameter is randomly sampled from the parameter ranges given in Tables S1 and S2. In the control case, the ejecta weathering is absent, and the surface temperature is moderate or even hot (Figure 3b), and $p\text{CO}_2$ is higher than the modern level (Figure 3a) to compensate the faint young Sun. The relatively high $p\text{CO}_2$ results in an oceanic pH lower than the modern value (Figure 3c). Also, the dissolved inorganic carbon (DIC) and carbonate alkalinity (ALK) in the ocean are larger than the modern values (Figures 3d and 3e). These features are due to the carbonate-silicate cycle and consistent with the results of Krissansen-Totton et al. (2018).

In contrast, as exemplified with Figure 2, the $p\text{CO}_2$ and surface temperature of the standard case (with impact ejecta) tend to be lower than those of the control case (Figures 3a and 3b). This is because the ejecta weathering is a sink of CO_2 , as explained above.

The relatively low $p\text{CO}_2$ results in a comparatively high ocean pH (Figure 3c). However, the ocean pH is constrained to be smaller than the threshold pH of 9 as shown in Figure 3c. This is because if ocean pH becomes larger than the threshold, the ejecta weathering stops, which prevents a further decrease in $p\text{CO}_2$ and a further increase in ocean pH .

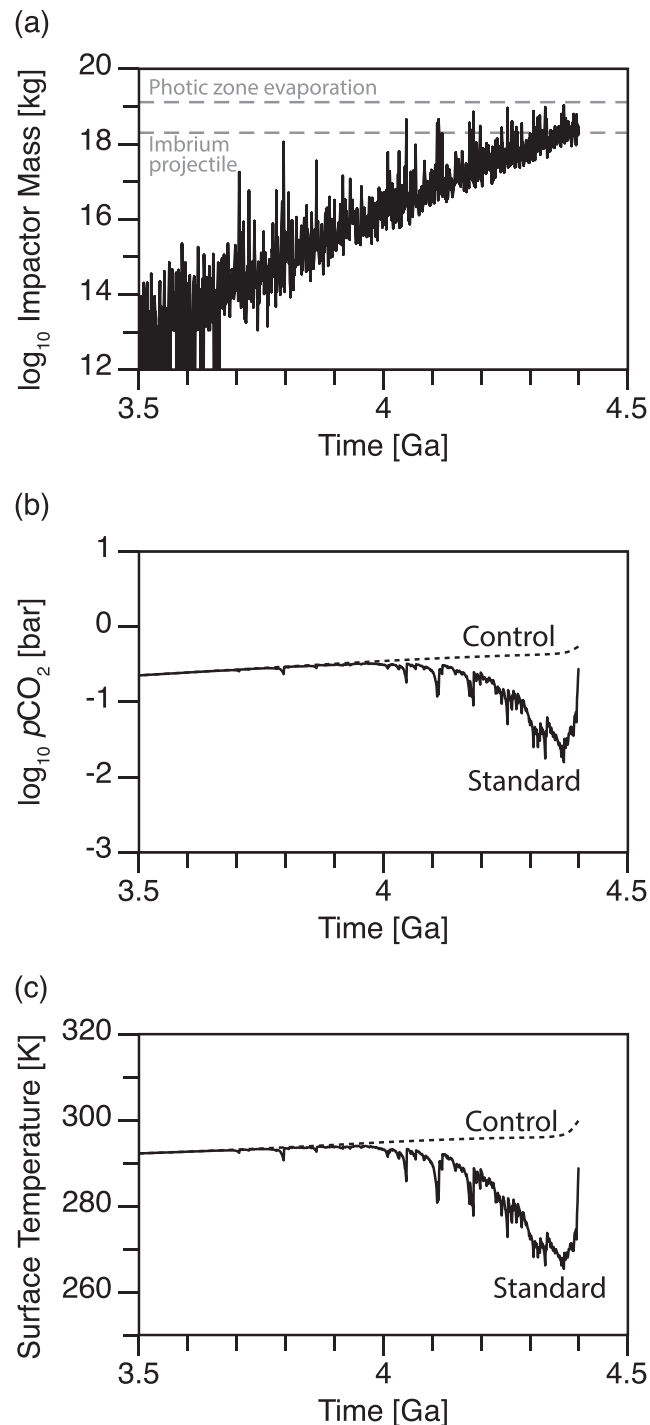


Figure 2. Imposed impactor mass, pressure of atmospheric CO₂ ($p\text{CO}_2$), and surface temperature as a function of time for a parameter set. The black solid line represents the surface temperature of the case with an ejecta weathering (i.e., the standard case). On the other hand, the black dotted line represents that of the case without the ejecta weathering (i.e., the control case). In addition, the dashed lines represent the impactor mass which evaporates a photic zone of ocean (e.g., 1.3×10^{19} kg; Sleep et al., 1989), and which corresponds to the projectile that made the Imbrium crater on Moon (e.g., 2×10^{18} kg; Baldwin, 1987). For both calculations of the standard and control cases, the same parameter set is applied. After a large impact (a), $p\text{CO}_2$ (b) and surface temperature (c) decreases.

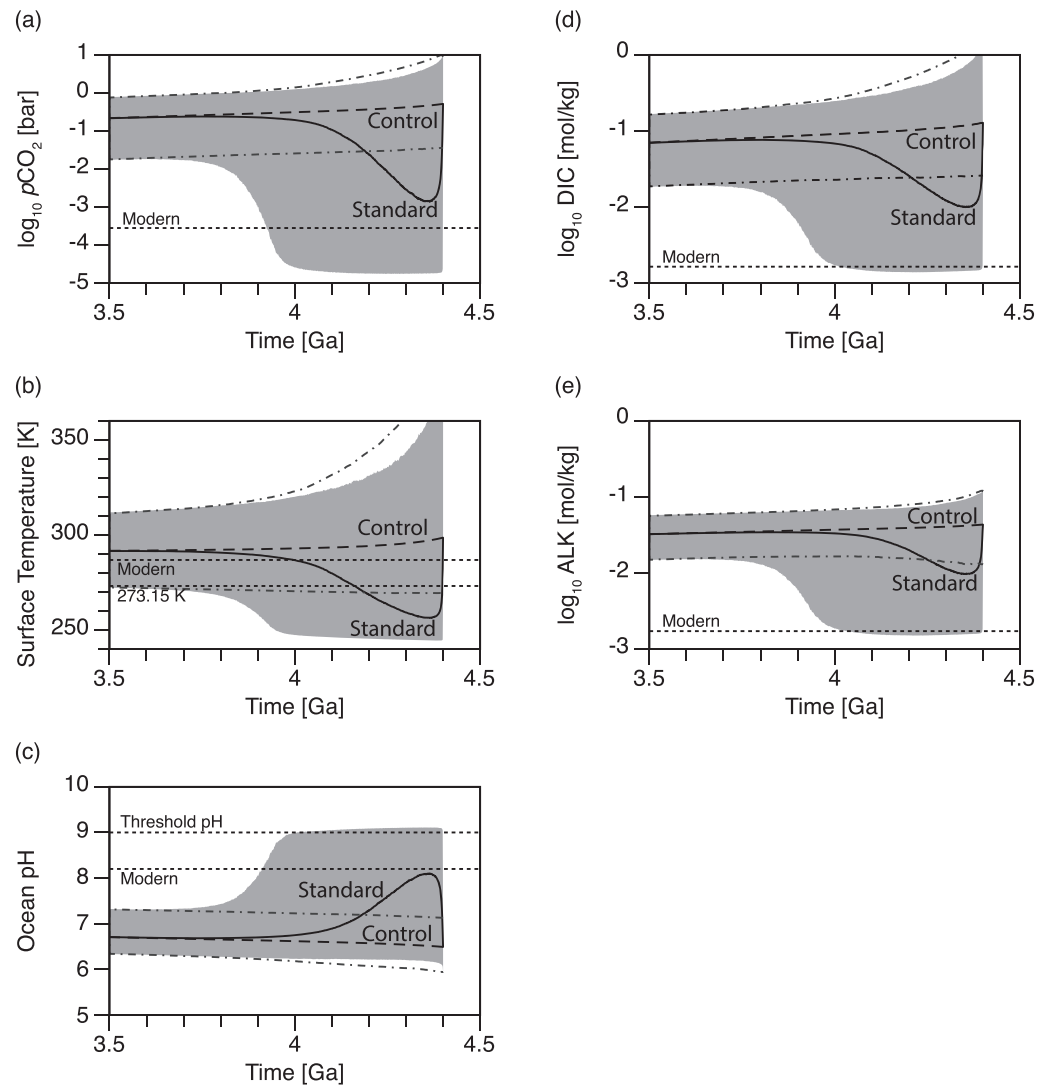


Figure 3. Standard case evolution: (a) $p\text{CO}_2$, (b) surface temperature, (c) ocean pH, (d) dissolved inorganic carbon (DIC) in ocean, and (e) carbonate alkalinity (ALK) in ocean. The units are bar for $p\text{CO}_2$, K for temperature, and mol/kg for DIC and ALK. The black solid line and gray shaded region represent the median value and 95% confidence interval of the standard case (i.e., with ejecta weathering), respectively. On the other hand, the black dashed line and dash-dot line represent the median value and 95% confidence interval of the control case (i.e., without ejecta weathering), respectively.

The DIC and ALK of the standard case also tend to be lower than those of the control case (Figures 3d and 3e). These features might appear counterintuitive because ejecta weathering is a source of carbonate alkalinity, ALK. However, the explanation is relatively straightforward. The increase in alkalinity following an impact is rapidly removed by carbonate precipitation and an adjustment of the carbonate system to higher pH, which causes a further increase in carbonate precipitation. The result is a low ALK on timescales of 10^3 to 10^6 years, during which time another impactor hits, maintaining the overall state of the ocean chemistry. The evolution of ALK, DIC, and $p\text{CO}_2$ can be understood in detail by examining what happens after a single impact, as described in section S2.

Returning to a general overview, in the early Hadean (~ 4.4 Ga), the differences between the standard and control cases are large. Then, the differences gradually shrink with time and disappear after 3.8 Ga (Figure 3). This trend is due to the decrease in the impact flux, which also decreases the ejecta production (Figure 1).

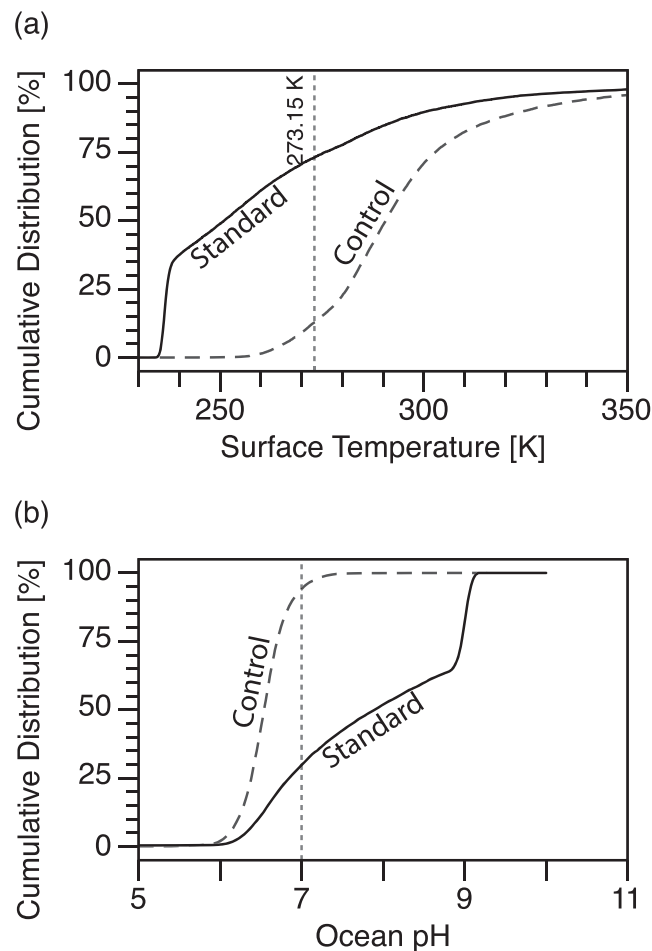


Figure 4. Cumulative distribution of (a) surface temperature and (b) ocean pH at 4.3 Ga. Black solid lines represent the case with the ejecta weathering (i.e., the standard case). On the other hand, black dashed lines represent the case without the ejecta weathering (i.e., the control case). As discussed in section 3, since the ejecta weathering decreases $p\text{CO}_2$, the surface temperature of the standard case is lower than that of the control case (a). And the ocean pH of the standard case is higher than that of the control case (b). Besides, for the standard case, the probability of the surface temperature below 273.15 K and the probability of the ocean pH above 7 are around 70%.

4. Discussion

4.1. A Cold Climate and Alkaline Surface Waters During the Hadean

As discussed in section 3, the ejecta weathering resulting from meteorite impacts causes relatively low surface temperature and high ocean pH. This point is highlighted in Figure 4, which shows the cumulative distribution of surface temperature (Figure 4a) and ocean pH (Figure 4b) at 4.3 Ga.

The surface temperature of the case without the ejecta weathering (i.e., the control case) is generally higher than 273.15 K as indicated by the black dashed line in Figure 4a. In contrast, the surface temperature of the case with the ejecta weathering (i.e., the standard case) is lower than that of the control case (Figure 4a). In particular, the probability that the surface temperature is less than 273.15 K is 67% at 4.3 Ga. Thus, the climate at 4.3 Ga was probably cold as a result of the consumption of CO_2 by ejecta weathering.

Similarly, the ocean pH of the control case is generally less than 7 as indicated by the dashed line in Figure 4b. In contrast, the ocean pH of the standard case is higher than that of the control case, and the probability that the ocean pH is higher than 7 is 70% at 4.3 Ga. Thus, the ocean at 4.3 Ga was probably weakly alkaline considering the ejecta weathering. There are no empirical constraints on the pH of the Hadean ocean and the oldest constraint is from ~ 3.7 Ga. At that time, the pattern of rare earth elements (REEs) in banded iron formations is consistent with precipitation from circumneutral to alkaline seawater in which carbonate ions

preferentially complexed the heavy REEs (Friend et al., 2008). At 3.7 Ga, our model result for ocean pH is consistent, within uncertainties, with this pH inference from data.

The low surface temperature and the high ocean pH both result from low $p\text{CO}_2$. On land, the low atmospheric $p\text{CO}_2$ could also allow neutral to weakly alkaline lakes in addition to the weakly alkaline ocean, because rivers flowing into lakes and the weathering of surrounding rocks would supply alkalinity, as today. This is important because carbonate-rich lakes with basic pH have been proposed as sites for the origin of life (Bada & Korenaga, 2018), in part because such aqueous chemistry concentrates critical reactants for prebiotic schemes, such as cyanide (Toner & Catling, 2019) and phosphate (Toner & Catling, 2019). Moreover, the concentration of cyanide is favored at lower temperature (Toner & Catling, 2019), while critical biomolecules, such as nucleobases, are known to be more stable at lower temperatures (Bada & Lazcano, 2002). In particular, eutectic conditions in frozen ice greatly extend the lifetime of ribozyme polymerase activity, promoting RNA replication and assembly in a so-called “cold RNA World” (e.g., Monnard & Szostak, 2008; Attwater et al., 2010). Thus, our model results support hypotheses that the origin of life occurred during a cool, quiescent mean climate state of the Hadean that existed between impacts. Such a state would occur after any fully ocean-vaporizing impacts, which were probably confined to before ~ 4.3 Ga (Marchi et al., 2014).

4.2. Robustness of Results

4.2.1. Uncertainty of the Randomly Sampled Parameters

During the Hadean, the surface temperature mainly depends on the CO_2 degassing rate and impact flux, that is, the production rate of impact ejecta, as explained in section S3. This is because the carbon cycle during the Hadean is mainly controlled by impact ejecta weathering as also shown in previous studies (Sleep & Zahnle, 2001; Zahnle & Sleep, 2002). Hence, a conservative range for parameters in the model (e.g., for abiotic weathering) does not affect the overall results for the Hadean.

We follow the CO_2 degassing model of Krissansen-Totton et al. (2018). In the model, CO_2 degassing rate depends on heat flow (see equation (S6)), which implicitly includes the dependency of CO_2 degassing of seafloor weathering and/or melt production depth. On the other hand, CO_2 is supplied from mid-ocean ridges and arc volcanoes, and CO_2 degassing should also depend on the carbon reservoir size of the mantle and/or oceanic crust (e.g., Sleep & Zahnle, 2001). Nonetheless, the results of Sleep and Zahnle (2001) and of Krissansen-Totton et al. (2018) are in good agreement with each other according to Krissansen-Totton et al. (2018). Thus, the evolution of the reservoir size of the mantle and/or oceanic crust would affect results less. The effect of recycling of carbon via arc volcanism is also discussed in section S7.

Since the timescale of the carbon cycle is relatively short ($< \sim 10^6$ year), the surface environment is in a steady state for a timescale of $> \sim 10^7$ year. Thus, we can regard an evolution of surface environment as an evolution of the steady state of the surface environment under a long timescale of $> 10^7$ year. Hence, the evolutionary range of surface environment depends on the range of parameters, such as of CO_2 degassing rate, rather than on each evolution of the parameters.

We set the range of CO_2 degassing rate so as that the evolutionary range of the CO_2 degassing rate covers the estimate by previous works (Godderis & Veizer, 2000; Holland, 2009; Korenaga, 2006; Zahnle & Sleep, 2002) as shown in Figure S1. We set the range of impact flux following the estimate based on lunar cratering (Sleep et al., 1989).

4.2.2. Effect of Plate Tectonics

In this study, we implicitly assume some style of plate tectonics. However, it is still uncertain when plate tectonics started (e.g., Korenaga, 2013). In terms of the carbon cycle, plate tectonics causes (1) continuous supply of carbon (i.e., CO_2 degassing) and (2) continuous supply of alkalinity through the production and weathering of seafloor and mountains and volcanoes on land. Since Hadean meteorite impacts would massively supply the source of alkalinity via weathered impact ejecta, the second point is unimportant even if the plate tectonics did not exist.

The CO_2 degassing rate before the plate tectonics is uncertain. For example, Foley and Smye (2018) examined the CO_2 degassing rate for a stagnant-lid planet, showing that an initial CO_2 degassing rate can be higher by an order of magnitude than the CO_2 degassing of the modern Earth. Note that this value is consistent with the range of this study (see Figure S1). Kite et al. (2009) also suggested that the degassing rate is even higher for a stagnant-lid planet than for a plate-tectonics planet during their early evolution, because of higher

mantle temperature of the stagnant-lid planet. If it is true, the surface temperature before the plate tectonics might be higher than we estimated.

4.2.3. Initial Conditions

We start the calculation with a moderate amount of $p\text{CO}_2$ (e.g., Figure 3). On the other hand, according to Sleep (2018), the Moon-forming impact resulted in an atmosphere containing 100 bar of CO_2 , which corresponds to 200 °C of surface temperature. The massive CO_2 atmosphere would remain until the atmospheric CO_2 subducts into the mantle as carbonate, which may take tens of millions of years or longer. Consequently, the initial conditions for our model assume that the transitional interval of high CO_2 and surface temperature after the Moon-forming impact has ended. We do not explicitly model the aftermath of the Moon-forming impact.

4.3. Possibility of a Snowball Earth During the Hadean

As shown above, a possibility that the surface temperature (T) is less than 273.15 K is around 70% at 4.3 Ga (Figure 4a) and more than 50% between 4.4 and 4.2 Ga (Figure 3b).

However, a surface temperature below 273.15 K does not always mean that the Earth is globally ice covered (i.e., a snowball Earth) because the surface temperature only represents the globally averaged temperature. For example, the threshold mean global temperature for the snowball Earth varies from ~ 240 K (Shields et al., 2013) to ~ 260 K (Paradise & Menou, 2017oct, 2017oct). The possibility of $T < 260$ K is 51% at 4.3 Ga (Figure 4). Thus, a permanent snowball Hadean Earth resulting from ejecta weathering would be unlikely, but the Hadean Earth was probably relatively cold.

Here, note that we neglect a shielding effect of dust produced by meteorite impacts. This is because the residence time of the dust (Holton et al., 1995; Pierazzo et al., 2003, 2 to 10years) is much shorter than the timescale of the carbon cycle ($\sim 10^6$ year) and hence would have little effect on the long-term evolution. The dust injected into the stratosphere shields sunlight because of its high albedo, resulting in a decrease in the surface temperature (e.g., Brugger et al., 2017). A decrease in the surface temperature might trigger the snowball event. Hence, there is a possibility that meteorite impacts cause a Hadean snowball event via the shielding effect of dust.

4.4. Stability and Duration of a Snowball Earth During the Hadean

Nonetheless, the Hadean Earth could enter a snowball state because of a large amount of impact ejecta, so it is worth considering the stability of a snowball state. Continental silicate weathering stops during a so-called “hard” snowball state of total ice cover, resulting in the accumulation of atmospheric CO_2 , which eventually melts global ice sheets (e.g., Hoffman et al., 1998). However, if the CO_2 degassing rate is relatively low (or the sink of CO_2 is relatively large), a planet returns to a snowball state and oscillates between the snowball state and nonsnowball state, which is known as a snowball limit cycle (Haqq-Misra et al., 2016; Kadoya & Tajika, 2014; Menou, 2015).

We can consider whether such a limit cycle might occur. First, suppose a hard snowball state happens, gas exchange between the atmosphere and ocean stops, and the ocean pH remains high. Because of the faint young Sun, the threshold $p\text{CO}_2$ to melt the global ice sheet is high (~ 0.1 bar) during the Hadean. If we take the CO_2 degassing rate during the Hadean to be roughly 10^{-7} to 10^{-5} bar per year, the duration of a snowball state is $\sim 10^4$ to 10^6 year. Since the duration of a nonsnowball state tends to be much shorter than that of the snowball (e.g., Kadoya & Tajika, 2014), the period of the snowball limit cycle during the Hadean is also 10^4 to 10^6 year. On the other hand, impact ejecta is lost in a timescale of $\sim 10^8$ year, that is, the timescale of seafloor resurfacing. So the amount of ejecta would be preserved during the snowball state. Therefore, if the amount of impact ejecta was large enough to result in a snowball state, the Earth might experience the snowball limit cycle.

Second, suppose a “soft” snowball state occurs, where CO_2 exchanges between the ocean and atmosphere because of incomplete ice cover. In this case, atmospheric CO_2 dissolves into oceans, which decreases the ocean pH so that CO_2 is removed as a consequence of seafloor and/or ejecta weathering. Hence, the duration of a soft snowball state would be longer than that of the hard snowball case (i.e., longer than 10^4 to 10^6 year). Hence, a soft snowball limit cycle would be unlikely, and such a state might persist if open water can be maintained.

In fact, Hadean impacts could create open water and maintain a soft snowball state. Open waters of 10^3 km^2 allow CO_2 to dissolve efficiently into the ocean (Le Hir et al., 2008). Assuming that the thickness of an ice

sheet is 1 km, the energy necessary to melt this ice sheet (i.e., $1 \times 10^3 \text{ km}^3$) is $\sim 3 \times 10^{17} \text{ kJ}$, and the energy necessary to raise the temperature of such an ice sheet to the melting temperature is $\sim 4 \times 10^{15} \text{ kJ/K}$. Hence, the energy to make open waters large enough for gas exchange is $\sim 10^{17}$ to 10^{18} kJ . If we assume that 50% of energy is used for the melting of ice sheet, following Sleep et al. (1989), and assume a velocity 20 km/s, an impact making such open waters corresponds to 10^{12} to 10^{13} kg (equivalent to an asteroid ~ 0.9 to 1.9 km across). Since the average impact flux is $\sim 10^{12}$ to 10^{13} kg/year during the Hadean (Sleep & Zahnle, 2001), open waters large enough for gas exchange are plausible during the Hadean.

Therefore, even if weathering of impact ejecta made the Earth a “hard” snowball state, subsequent impacts would create open waters, allowing atmospheric CO_2 to dissolve into the ocean. The dissolution of CO_2 would prevent the Earth from recovering from such a “soft” snowball state. Consequently, it is possible that the early Hadean Earth got locked into a “soft” snowball state, at least until the impact flux declined. The total impact flux in kg/year is shown in Figure 1, and the mass tends to be dominated by the largest single impactor (Tremaine & Dones, 1993). The flux drops below a median value of $\sim 10^{12} \text{ kg/year}$ in a 2-sigma range of time from 4.4 to 4.0 Ga. The median time is 4.3 Ga, so a “soft” snowball state, if it existed, would mostly likely cease in the early Hadean.

4.5. Effect of Continental Size

The amount of land affects continental weathering, and in the extreme case of no land, there is no continental weathering and the possibility of a warmer climate. Without land, the loss of carbon in seafloor weathering is the only long-term feedback on climate, and this is a weaker feedback than continental weathering (Krissansen-Totton et al., 2018). In a case excluding continental weathering (a “no-land” case), our model produces a surface temperature that tends to be larger than that of the standard case (Figure S5). This is similar to the results of Krissansen-Totton et al. (2018), who found that the surface temperature increased by $\sim 15 \text{ K}$ compared to a case including continental weathering. In our model, at 3.5 Ga, the surface temperature of the no-land case is larger by $13.7^{+28.9}_{-12.9} \text{ K}$ [2σ] than that of the standard case, which in good agreement with the results of Krissansen-Totton et al. (2018) (see Figure S6). Our model includes impact ejecta (unlike that of Krissansen-Totton et al., 2018), but by 3.5 Ga, the effect of ejecta weathering can be ignored (see also section 3).

In the early Hadean, the difference in the surface temperature at 4.3 Ga of a case without land versus that with land is $7.2^{+32.6}_{-14.2} \text{ K}$ [2σ] (Figure S6). If we exclude ejecta weathering, the difference at 4.3 Ga increases to $19.2^{+58.0}_{-19.5} \text{ K}$ [2σ] (Figure S6). Thus, ejecta weathering suppresses the effect of zero continental size during the early Hadean.

The small effect of continental size is because during the early Hadean there is a high ejecta production rate, so CO_2 degassing is mainly balanced with ejecta weathering, not with the continental silicate weathering (see Figure S7). Hence, the continental size and associated continental weathering rates have less effect on $p\text{CO}_2$ and surface temperature.

4.6. Late Heavy Bombardment

The cold and alkaline ocean due to ejecta weathering is confined in the early Hadean (Figure 3). This is because we assumed an exponential and monotonic decrease in the impact flux (Figure 1). On the other hand, some studies suggested that there was a spike of meteorite impact flux around 3.9–3.8 Ga, which is known as the late heavy bombardment (LHB) (e.g., Bottke & Norman, 2017), although it remains controversial whether or not the LHB exists (e.g., Hartmann, 2019) and how long the duration of the LHB was (e.g., Niihara et al., 2019; Zellner, 2017). Assuming the LHB, such an intense impact flux also results in a cold surface environment at 3.8 Ga (Charnay et al., 2017). In this study, we also consider the effect of LHB during the late Hadean and the early Archean.

Figure 5 compares the case where the LHB is included (hereafter, a “LHB” case) with the case where the average impact flux decreases monotonically (i.e., the standard case). Previous works (Anbar et al., 2001; Gomes et al., 2005) estimated the mass delivered to the Earth during the LHB was $\sim 2 \times 10^{20} \text{ kg}$. Hence, we set the average impact flux of the LHB case at $6.7 \times 10^{11} \text{ kg/year}$ between 3.8 and 4.1 Ga (Figure 1).

As pointed out in Charnay et al. (2017), the LHB also results in a relatively low $p\text{CO}_2$ and surface temperature (Figures 5a and 5b). In addition, the ocean pH is relatively high during the LHB (Figure 5c).

Furthermore, although we assumed that the impact flux decreases abruptly at 3.8 Ga (Figure 1), the cold and alkaline ocean lasts even after 3.8 Ga. This is because the impact ejecta accumulated during the LHB

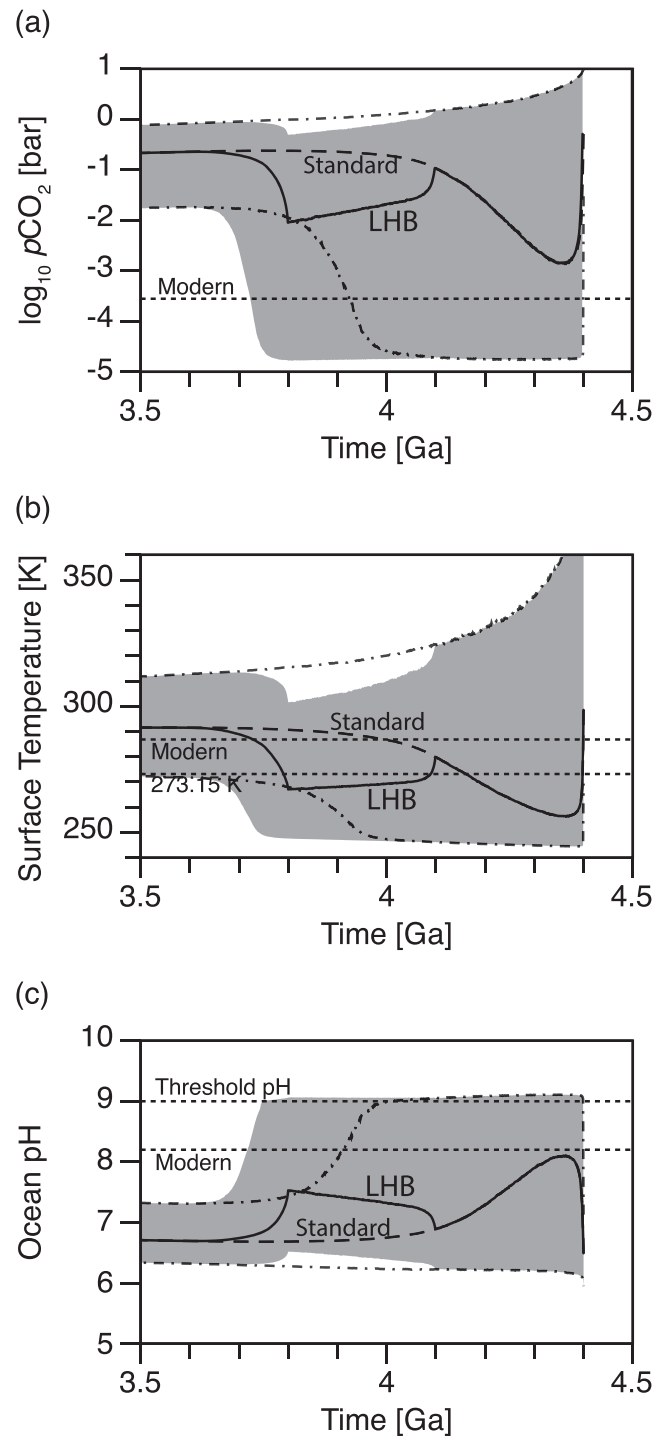


Figure 5. Effect of the late heavy bombardment (LHB). Black solid line and gray shaded region represent the median value and 95% confidence interval for the case with LHB. Here, we assumed that the impact flux increased between 3.8 and 4.1 Ga (see also Figure 1). On the other hand, black dashed line and dash-dot line represent the median value and 95% confidence interval for the standard case (see also Figure 3).

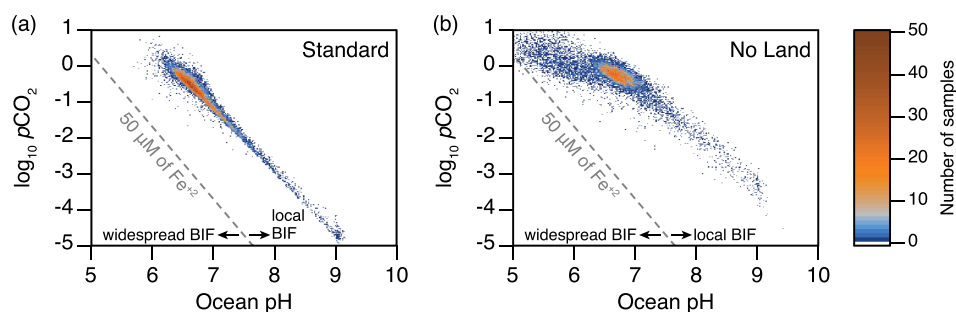


Figure 6. Distribution of $p\text{CO}_2$ and ocean pH at 3.8 Ga, obtained by 10,000 times sampling: (a) the standard case (see also Figures 3a and 3c) and (b) the no-land case (see also Figures S5a and S5c). The gray dashed line represents the condition that a concentration of Fe^{2+} is $50 \mu\text{M}$, which is the threshold for a widespread banded iron formation (BIF) (Song et al., 2017). Here, we assume a saturation of siderite (i.e., $\text{FeCO}_3 + 2\text{H}^+ \rightarrow \text{Fe}^{2+} + \text{CO}_2 + \text{H}_2\text{O}$). The $p\text{CO}_2$ and ocean pH are out of the condition of BIF.

remains for a while even after the decrease in the impact flux. Since the impact ejecta also decreases via seafloor resurfacing and loss to the mantle (equation (2)), the amount of the impact ejecta would decrease on the timescale of seafloor resurfacing ($\sim 10^8$ year). Therefore, the timescale of the effect of the impact ejecta after the LHB does not exceed the $\sim 10^8$ year.

4.7. Effect of Other Greenhouse Gases

The atmosphere of the early Earth from the Hadean to the Archean, which would be more reducing than the present, might contain greenhouse gases, such as NH_3 , CH_4 , and H_2 (e.g., Sagan, 1977). However, the partial pressure of NH_3 would be very small because of photodissociation of NH_3 (e.g., Kasting, 1982) though there is still a possibility that organic haze could shield NH_3 from ultraviolet light (Sagan & Chyba, 1997). The amount of atmospheric CH_4 would also be small during the prebiotic Hadean because of a lack of biogenic CH_4 (Kasting & Catling, 2003).

However, the primordial atmosphere of the Earth might contain a large amount of H_2 depending upon the redox state of the early Hadean mantle. Moreover, the atmosphere might also contain larger amount of N_2 than the present (Goldblatt et al., 2009). According to Wordsworth and Pierrehumbert (2013), if the atmosphere contains three times of the present level of N_2 and 10% of H_2 , the surface temperature increases by roughly 10 to 20 K due to a H_2 - N_2 collision induced absorption (CIA) (see also Figure S14). For example, if the surface temperature increases by 20 K compared to the standard case (i.e., Figure 3b), the probability of the surface temperature below 273.15 K at 4.3 Ga to $\sim 30\%$ (see also Figure 4a).

However, the negative feedback of carbon cycle decreases $p\text{CO}_2$ if there is an additional greenhouse effect other than of CO_2 (e.g., Krissansen-Totton et al., 2018). Hence, the net increase of the surface temperature by the H_2 - N_2 CIA would be suppressed. In addition, the decrease in $p\text{CO}_2$ would result in surface waters with basic pH. Moreover, the amounts of H_2 and N_2 during the Hadean are still uncertain. Therefore, the cold and alkaline surface environment would remain likely.

4.8. Archean Banded Iron Formation

A banded iron formation (BIF) is present around 3.8 Ga in Isua in western Greenland (e.g., Bekker et al., 2014). The BIF might indicate that the ocean contained a significant concentration of Fe^{2+} , which was higher than $50 \mu\text{M}$ (Song et al., 2017). Since the solubility of Fe^{2+} depends on a concentration of CO_3^{2-} and pH, the existence of BIF might give a constraint on $p\text{CO}_2$ and ocean pH. On the other hand, Polat and Frei (2005) suggests that iron leached from the oceanic crust and was redeposited by hydrothermal fluid. In such a case, the BIF would indicate a local condition rather than the average condition of the ocean.

Figure 6 shows the distribution of $p\text{CO}_2$ and ocean pH, which was obtained by sampling 10,000 times. In addition, the gray dashed line indicates a concentration of Fe^{2+} of $50 \mu\text{M}$, assuming siderite precipitation (i.e., $\text{FeCO}_3 + 2\text{H}^+ \rightarrow \text{Fe}^{2+} + \text{CO}_2 + \text{H}_2\text{O}$). As shown in Figure 6, the ocean pH is so high that the concentration of Fe^{2+} under siderite saturation is lower than the threshold of the widespread BIF (i.e., $50 \mu\text{MFe}^{2+}$). The situation does not differ in the no-land case, where the ocean pH tends to be lower than that of the standard case (Figure 6b). Hence, the average condition of the ocean might not be suitable for the BIF. This would

be supportive of deposition of BIF via hydrothermal alteration and local conditions of pH and redox rather than those of the average, global bulk ocean.

4.9. Advantage of Cold Hadean Conditions and Low $p\text{CO}_2$ for the Origin of Life

Whether the origin of life occurred in a hydrothermal vent, ocean, or a pond on a land is much debated (e.g., Stüeken et al., 2013). In general, organic chemists tend to favor a surface environment for prebiotic chemistry because under such conditions nucleotides, amino acids, and lipid precursors have been synthesized in the laboratory, whereas no similar synthesis in hydrothermal vent conditions has been done (Ritson et al., 2018). The photostability of the bases in RNA and DNA (i.e., cytosine, thymine, uracil, adenine, and guanine) may indicate that these bases were selected by ultraviolet radiation of the Sun from other alternatives that are less photostable (Mulkiđjanian et al., 2012). Mat et al. (2008) suggests that life arose with RNA under psychrophilic to mesophilic conditions, then propagated to and survived under thermophilic to hyperthermophilic conditions. Here, early life obtained DNA (a “hot cross origin of life” hypothesis) based on phylogenetic analyses coupled with thermal stability of DNA and RNA, and a limit via carbon fixation.

The results of this study, showing a high probability of a cold Hadean, may have some advantages for a surface environment for the origin of life. As mentioned previously, a cold temperature is favorable for the stability of critical biomolecules, such as RNA, which survives better at low temperatures (Bada & Lazcano, 2002). Also, eutectic freezing could result in a high concentration of prebiotic ingredients in an ice matrix (e.g., Kitadai & Maruyama, 2018). Hence, the low surface temperatures modeled in this study could be advantageous.

The relatively low $p\text{CO}_2$ (e.g., Figure 3a) would allow alkaline lakes on land, as today. According to Cleaves et al. (2008), acidic conditions promote oxidative decomposition of amino acids, so that alkaline pH increases the yield of amino acids. In addition, cold, carbonate-rich lakes (with quasi-neutral to basic basic) concentrate cyanide and phosphate (Toner & Catling, 2019; 2019), which are essential reagents for prebiotic schemes that have had considerable success in recent years in making biomolecules with relatively high yield and specificity (Islam & Powner, 2017).

Here, note that an alkaline environment can locally exist: for example, serpentinization (e.g., $2\text{Mg}_2\text{SiO}_4 + 3\text{H}_2\text{O} \rightarrow \text{Mg}_3\text{Si}_2\text{O}_5(\text{OH})_4 + \text{Mg}(\text{OH})_2$) can create a local alkaline environment in a lake or aquifer (Benner et al., 2010, 2012). Hence, a global condition of basic pH due to low $p\text{CO}_2$, which this study indicates, might not always be necessary for the origin of life. Nonetheless, the cold and alkaline surface environment due to ejecta weathering might be supportive of the origin of life.

4.10. Effect on the Habitable Zone of Other Earth-Like Planets

Because of the way planets are formed by accretion, an exoplanet would also experience intense meteorite impacts in its early history. According to some studies (e.g., Lisse et al., 2012), there is even a possibility of the late heavy bombardment. Hence, an exoplanet might also experience an early cold surface environment and even an early snowball state.

Snowball states can affect the width of the habitable zone (HZ) in extrasolar systems. A planet that has a carbonate-silicate cycle should shift to a warm state after a snowball state because of atmospheric CO_2 that accumulates when continental weathering ceases to melt the ice sheet (Hoffman et al., 1998). However, recent studies suggest that under a low insolation even within the HZ limits, such a recovery from a snowball state is prevented owing to the condensation of CO_2 ice (Turbet et al., 2017) and/or ice albedo feedback (Kadoya & Tajika, 2019). This indicates that the insolation needed at the outer limit of the HZ is higher (i.e., the HZ is narrower) than previous estimates (Kasting et al., 1993; Kopparapu et al., 2013) if a snowball planet is common.

Therefore, intense meteorite impacts, acting within the context of a carbonate-silicate cycle on a rocky world, might cause the location of the outer limit of the habitable zone to move inward.

5. Conclusions

In this study, we modeled the evolution of the surface environment of the Earth, including the mean global surface temperature, atmospheric $p\text{CO}_2$, and oceanic pH. We used a carbonate-silicate model that includes the weathering of impact ejecta, continental weathering, seafloor weathering, and seawater car-

bonate chemistry. To the extent possible, weathering and other parameterizations use the best available empirical justifications. Parameter ranges in the model are randomly sampled and multiple runs are done to build up statistics.

Results for the Archean Earth are consistent with previous studies (e.g., Charnay et al., 2017; Krissansen-Totton et al., 2018) and show that the surface environment had moderate surface temperature, for example, $291.7^{+19.7}_{-19.3}$ K at 3.5 Ga, and moderately high $p\text{CO}_2$ levels, for example, $\log_{10}p\text{CO}_2$ [bar] is $-0.66^{+0.54}_{-1.09}$ at 3.5 Ga. The moderation of climate and associated modulation of $p\text{CO}_2$ is a result of negative feedbacks on surface temperature and $p\text{CO}_2$ from continental and seafloor weathering in the carbonate-silicate cycle.

In contrast, during the Hadean, most model realizations produce low $p\text{CO}_2$ and surface temperature with a lower number of runs producing high $p\text{CO}_2$ and moderate surface temperatures like those during the Archean. For example, at 4.3 Ga, $\log_{10}p\text{CO}_2$ [bar] is $-2.54^{+3.01}_{-2.21}$, and surface temperature is $259.2^{+84.1}$ K. The probability of a cold surface environment below freezing point in the early Hadean is high, approximately 70% at 4.3 Ga. This result is due to the weathering of ejecta from intense meteorite impact bombardment. Such a cold surface environment is consistent with the results of Sleep and Zahnle (2001) and Zahnle and Sleep (2002). However, our model is different to that of Sleep and Zahnle (2001) because our model includes ocean chemistry, a more empirically justified treatment of the kinetics of seafloor weathering, and a Monte Carlo approach to assess probabilities.

Because of the inclusion of ocean chemistry, our model is able to simulate the pH of the early ocean. We find that the low $p\text{CO}_2$ (caused by acid weathering of impact ejecta) results in a neutral to weakly alkaline ocean, for example, $7.90^{+1.21}_{-1.69}$ at 4.3 Ga. Currently, there are no direct empirical constraints on the pH of the Hadean ocean. The oldest inference about seawater pH comes from rare earth element (REE) distributions in ~ 3.7 Ga banded iron formation units in Isua, West Greenland. These data suggest that REEs precipitated from seawater in which heavy REEs were preferentially complexed with carbonate ions, which requires seawater pH that was circumneutral to alkaline (Friend et al., 2008). Thus, the earliest empirical inferences are consistent with our model results, within uncertainty.

Cold conditions in the Hadean and moderate levels of $p\text{CO}_2$ are favorable for hypotheses of an origin of life on land. Lakes on volcanic islands have been proposed as sites for the origin of life (Bada & Korenaga, 2018). Such environments readily overcome the “concentration problem” for prebiotic chemistry, in which reactants must be sufficiently concentrated to drive reactions, because lakes can evaporate or, in a cold environment, lakes can freeze and concentrate solutes in residual water.

One critical reactant for prebiotic chemistry is cyanide because cyanide can repeatedly add C-N moieties to organic molecules, allowing the buildup of long biomolecules, including amino acids, ribonucleotides, and lipid precursors (Canavelli et al., 2019; Islam & Powner, 2017; Sutherland, 2016). Thermodynamics favors the concentration of cyanide in low temperature aqueous solutions (Toner & Catling, 2019). In addition, biomolecules that are needed for the origin of life, such as nucleobases, are more stable at low temperatures (Bada & Lazcano, 2002), and eutectic phases in ice promote RNA self-replication of a so-called “cold RNA World” (Attwater et al., 2010).

The coldest environment and most alkaline ocean conditions produced by our model are confined to the early Hadean when the impact flux and associated ejecta production rate were high. However, impact craters on the Moon also indicate the possibility of an enhanced impact flux around 3.8 Ga, the late heavy bombardment (LHB) (e.g., Niihara et al., 2019), although the LHB hypothesis has been challenged recently (Hartmann, 2019; Zellner, 2017). In the traditional LHB model, the estimated impact flux is high enough to result in a cold and alkaline ocean in the early Archean (e.g., $267.0^{+34.6}_{-19.5}$ K and $\text{pH}7.53^{+1.53}_{-1.01}$ at 3.8 Ga). Hence, there is also the possibility that early life in the Archean evolved in a cold and alkaline ocean.

Acknowledgments

We thank Norm Sleep and an anonymous reviewer for constructive reviews. Funding was provided by the Simons Collaboration on the Origin of Life Grant 511570 awarded to DCC and NASA Exobiology Grant NNX15AL23G. Source code and data used in this research are available on zenodo (doi: <https://doi.org/10.5281/zenodo.3579610>).

References

- Anbar, A. D., Zahnle, K. J., Arnold, G. L., & Mojzsis, S. J. (2001). Extraterrestrial iridium, sediment accumulation and the habitability of the early earth's surface. *Journal of Geophysical Research*, 106(E2), 3219–3236. <https://doi.org/10.1029/2000JE001272>
- Attwater, J., Wochner, A., Pinheiro, V. B., Coulson, A., & Holliger, P. (2010). Ice as a protocellular medium for RNA replication. *Nature Communications*, 1, 76. [https://doi.org/10.1038/ncomms1076\(2010\)](https://doi.org/10.1038/ncomms1076(2010))
- Bada, J., & Korenaga, J. (2018). Exposed areas above sea level on earth > 3.5 Gyr ago: Implications for prebiotic and primitive biotic chemistry. *Life*, 8(4), 55. <https://doi.org/10.3390/life8040055>

- Bada, J. L., & Lazcano, A. (2002). Some like it hot, but not the first biomolecules. *Science*, 296(5575), 1982–1983. <https://doi.org/10.1126/science.1069487>
- Baldwin, R. B. (1987). On the relative and absolute ages of seven lunar front face basins: II. From crater counts. *Icarus*, 71(1), 19–29. [https://doi.org/10.1016/0019-1035\(87\)90159-X](https://doi.org/10.1016/0019-1035(87)90159-X)
- Bekker, A., Planavsky, N. J., Krape, B., Rasmussen, B., Hofmann, A., Slack, J. F., et al. (2014). 9.18 - iron formations: Their origins and implications for ancient seawater chemistry. In H. D. Holland, & K. K. Turekian (Eds.), *Treatise on geochemistry (second edition)* (pp. 561–628). Oxford: Elsevier. <https://doi.org/10.1016/B978-0-08-095975-7.00719-1>
- Bell, E. A., Boehnke, P., Harrison, T. M., & Mao, W. L. (2015). Potentially biogenic carbon preserved in a 4.1 billion-year-old zircon. *Proceedings of the National Academy of Sciences*, 112(47), 14,518–14,521. <https://doi.org/10.1073/pnas.1517557112>
- Benner, S. A., Kim, H.-J., & Carrigan, M. A. (2012). Asphalt, water, and the prebiotic synthesis of ribose, ribonucleosides, and rna. *Accounts of Chemical Research*, 45(12), 2025–2034. <https://doi.org/10.1021/ar200332w>
- Benner, S. A., Kim, H.-J., Kim, M.-J., & Ricardo, A. (2010). Planetary organic chemistry and the origins of biomolecules. *Cold Spring Harbor perspectives in biology*, 2(7), a003467.
- Berner, R. A., & Kothavala, Z. (2001). Geocarb III: A revised model of atmospheric CO₂ over Phanerozoic time. *American Journal of Science*, 301(2), 182–204. <https://doi.org/10.2475/ajs.301.2.182>
- Boehnke, P., Bell, E. A., Stephan, T., Trappitsch, R., Keller, C. B., Pardo, O. S., et al. (2018). Potassic, high-silica Hadean crust. *Proceedings of the National Academy of Sciences*, 115(25), 6353–6356. <https://doi.org/10.1073/pnas.1720880115>
- Bottke, W. F., & Norman, M. D. (2017). The late heavy bombardment. *Annual Review of Earth and Planetary Sciences*, 45(1), 619–647. <https://doi.org/10.1146/annurev-earth-063016-020131>
- Boussau, B., Blanquart, S., Necseula, A., Lartillot, N., & Gouy, M. (2008). Parallel adaptations to high temperatures in the Archaean eon. *Nature*, 456(7224), 942. <https://doi.org/10.1038/nature07393>
- Brugger, J., Feulner, G., & Petri, S. (2017). Baby, it's cold outside: Climate model simulations of the effects of the asteroid impact at the end of the Cretaceous. *Geophysical Research Letters*, 44, 419–427. <https://doi.org/10.1002/2016GL072241>
- Buick, R. (2001). Life in the Archaean. In *Palaebiology II* (pp. 13–21). Oxford: John Wiley & Sons, Ltd. <https://doi.org/10.1002/9780470999295.ch3>
- Canavelli, P., Islam, S., & Powner, M. W. (2019). Peptide ligation by chemoselective aminonitrile coupling in water. *Nature*, 1371, 4. <https://doi.org/10.1038/s41586-019-1371-4>
- Cantine, M. D., & Fournier, G. P. (2018). Environmental adaptation from the origin of life to the last universal common ancestor. *Origins of Life and Evolution of Biospheres*, 48(1), 35–54. <https://doi.org/10.1007/s11084-017-9542-5>
- Catchpole, R. J., & Forterre, P. (2019). The evolution of reverse gyrase suggests a nonhyperthermophilic last universal common ancestor. *Molecular Biology and Evolution*, 36(12), 2737–2747. <https://doi.org/10.1093/molbev/msz180>
- Charnay, B., Le Hir, G., Fluteau, F., Forget, F., & Catling, D. C. (2017). A warm or a cold early Earth? New insights from a 3-D climate-carbon model. *Earth and Planetary Science Letters*, 474, 97–109. <https://doi.org/10.1016/j.epsl.2017.06.029>
- Cleaves, H. J., Chalmers, J. H., Lazcano, A., Miller, S. L., & Bada, J. L. (2008). A reassessment of prebiotic organic synthesis in neutral planetary atmospheres. *Origins of Life and Evolution of Biospheres*, 38(2), 105–115. <https://doi.org/10.1007/725s11084-007-9120-3>
- Collins, G. S., Melosh, H. J., & Marcis, R. A. (2005). Earth impact effects program: A web-based computer program for calculating the regional environmental consequences of a meteoroid impact on Earth. *Meteoritics & Planetary Science*, 40(6), 817–840. <https://doi.org/10.1111/j.1945-5100.2005.tb00157.x>
- Crovisier, J. L., Honnorez, J., & Eberhart, J. P. (1987). Dissolution of basaltic glass in seawater: Mechanism and rate. *Geochimica et Cosmochimica Acta*, 51(11), 2977–2990. [https://doi.org/10.1016/0016-7037\(87\)90371-1](https://doi.org/10.1016/0016-7037(87)90371-1)
- Foley, B. J., & Smye, A. J. (2018). Carbon cycling and habitability of earth-sized stagnant lid planets. *Astrobiology*, 18(7), 873–896. <https://doi.org/10.1089/ast.2017.1695>
- Franck, S., Kossacki, K. J., Von Bloth, W., & Bounama, C. (2002). Long-term evolution of the global carbon cycle: Historic minimum of global surface temperature at present. *Tellus B: Chemical and Physical Meteorology*, 54(4), 325–343. <https://doi.org/10.3402/tellusb.v54i4.16669>
- Friend, C. R. L., Nutman, A. P., Bennett, V. C., & Norman, M. D. (2008). Seawater-like trace element signatures (REE+Y) of Eoarchaean chemical sedimentary rocks from southern West Greenland, and their corruption during high-grade metamorphism. *Contributions to Mineralogy and Petrology*, 155(2), 229–246. <https://doi.org/10.1007/s00410-007-0239-z>
- Gaucher, E. A., Govindarajan, S., & Ganesh, O. K. (2008). Palaeotemperature trend for Precambrian life inferred from resurrected proteins. *Nature*, 451(7179), 704. <https://doi.org/10.1038/nature06510>
- Genda, H., Brasser, R., & Mojzsis, S. J. (2017). The terrestrial late veneer from core disruption of a lunar-sized impactor. *Earth and Planetary Science Letters*, 480, 25–32. <https://doi.org/10.1016/j.epsl.2017.09.041>
- Gislason, S. R., & Oelkers, E. H. (2003). Mechanism, rates, and consequences of basaltic glass dissolution: II. An experimental study of the dissolution rates of basaltic glass as a function of pH and temperature. *Geochimica et Cosmochimica Acta*, 67(20), 3817–3832. [https://doi.org/10.1016/S0016-7037\(03\)00176-5](https://doi.org/10.1016/S0016-7037(03)00176-5)
- Godderis, Y., & Veizer, J. (2000). Tectonic control of chemical and isotopic composition of ancient oceans; the impact of continental growth. *American Journal of Science*, 300(5), 434–461.
- Goldblatt, C., Claire, M. W., Lenton, T. M., Matthews, A. J., Watson, A. J., & Zahnle, K. J. (2009). Nitrogen-enhanced greenhouse warming on early Earth. *Nature Geoscience*, 2(12), 891.
- Gomes, R., Levison, H. F., Tsiganis, K., & Morbidelli, A. (2005). Origin of the cataclysmic late heavy bombardment period of the terrestrial planets. *Nature*, 435(7041), 466–469. <https://doi.org/10.1038/nature03676>
- Haqq-Misra, J., Koppurapu, R. K., Batalha, N. E., Harman, C. E., & Kasting, J. F. (2016). Limit cycles can reduce the width of the habitable zone. *The Astrophysical Journal*, 827(2), 120. <https://doi.org/10.3847/0004-637x/827/2/120>
- Hartmann, W. K. (2019). History of the terminal cataclysm paradigm: Epistemology of a planetary bombardment that never (?) happened. *Geosciences*, 9(7), 285. <https://doi.org/10.3390/geosciences9070285>
- Hoffman, P. F., Kaufman, A. J., Halverson, G. P., & Schrag, D. P. (1998). A Neoproterozoic snowball Earth. *Science*, 281(5381), 1342–1346. <https://doi.org/10.1126/science.281.5381.1342>
- Holland, H. D. (2009). Why the atmosphere became oxygenated: A proposal. *Geochimica et Cosmochimica Acta*, 73(18), 5241–5255.
- Holton, J. R., Haynes, P. H., McIntyre, M. E., Douglass, A. R., Rood, R. B., & Pfister, L. (1995). Stratosphere-troposphere exchange. *Reviews of Geophysics*, 33(4), 403–439. <https://doi.org/10.1029/95RG02097>
- Islam, S., & Powner, M. W. (2017). Prebiotic systems chemistry: Complexity overcoming clutter. *Chem*, 2(4), 470–501. <https://doi.org/10.1016/j.chempr.2017.03.001>

- Isson, T. T., & Planavsky, N. J. (2018). Reverse weathering as a long-term stabilizer of marine pH and planetary climate. *Nature*, *560*(7719), 471–475. <https://doi.org/10.1038/s41586-018-0408-4>
- Johnson, J. W., Oelkers, E. H., & Helgeson, H. C. (1992). SUPCRT92: A software package for calculating the standard molal thermodynamic properties of minerals, gases, aqueous species, and reactions from 1 to 5000 bar and 0 to 1000 C. *Computers & Geosciences*, *18*(7), 899–947. [https://doi.org/10.1016/0098-3004\(92\)90029-Q](https://doi.org/10.1016/0098-3004(92)90029-Q)
- Kadoya, S., & Tajika, E. (2014). Conditions for oceans on earth-like planets orbiting within habitable zone: Importance of volcanic CO₂ degassing. *Astrophysical Journal*, *790*(2), 107–113. <https://doi.org/10.1088/0004-637X/790/2/107>
- Kadoya, S., & Tajika, E. (2019). Outer limits of the habitable zone in terms of climate mode and climate evolution of earth-like planets. *Astrophysical Journal*, *875*(1), 7. <https://doi.org/10.3847/1538-4357/ab0aef>
- Kasting, J. F. (1982). Stability of ammonia in the primitive terrestrial atmosphere. *Journal of Geophysical Research: Oceans*, *87*(C4), 3091–3098. <https://doi.org/10.1029/JC087iC04p03091>
- Kasting, J. F., & Catling, D. (2003). Evolution of a habitable planet. *Annual Review of Astronomy and Astrophysics*, *41*(1), 429–463. <https://doi.org/10.1146/annurev.astro.41.071601.170049>
- Kasting, J. F., Whitmire, D. P., & Reynolds, R. T. (1993). Habitable zones around main-sequence stars. *Icarus*, *101*(1), 108–128. <https://doi.org/10.1006/icar.1993.1010>
- Kempe, S., & Degens, E. T. (1985). An early soda ocean? *Chemical Geology*, *53*(1-2), 95–108. [https://doi.org/10.1016/0009-2541\(85\)90023-3](https://doi.org/10.1016/0009-2541(85)90023-3)
- Kitadai, N., & Maruyama, S. (2018). Origins of building blocks of life: A review. *Geoscience Frontiers*, *9*(4), 1117–1153. <https://doi.org/10.1016/j.gsf.2017.07.007>
- Kite, E. S., Manga, M., & Gaidos, E. (2009). Geodynamics and rate of volcanism on massive Earth-like planets. *The Astrophysical Journal*, *700*(2), 1732–1749. <https://doi.org/10.1088/0004-637X/700/2/1732>
- Knoll, A. H., & Nowak, M. A. (2017). The timetable of evolution. *Science Advances*, *3*(5), 1–14. <https://doi.org/10.1126/sciadv.1603076>
- Kopparapu, R. K., Ramirez, R., Kasting, J. F., Eymet, V., Robinson, T. D., Mahadevan, S., et al. (2013). Habitable zones around main-sequence stars: New estimates. *Astrophysical Journal*, *765*(2), 16. <https://doi.org/10.1088/0004-637X/765/2/131>
- Korenaga, J. (2006). Archean geodynamics and the thermal evolution of Earth. *Archean geodynamics and environments* (pp. 7–32). Washington, DC: American Geophysical Union. <https://doi.org/10.1029/164GM03>
- Korenaga, J. (2013). Initiation and evolution of plate tectonics on earth: Theories and observations. *Annual Review of Earth and Planetary Sciences*, *41*(1), 117–151. <https://doi.org/10.1146/annurev-824earth-050212-124208>
- Krissansen-Totton, J., Arney, G. N., & Catling, D. C. (2018). Constraining the climate and ocean pH of the early earth with a geological carbon cycle model. *Proceedings of the National Academy of Sciences*, *115*(16), 4105–4110. <https://doi.org/10.1073/pnas.1721296115>
- Krissansen-Totton, J., & Catling, D. C. (2017). Constraining climate sensitivity and continental versus seafloor weathering using an inverse geological carbon cycle model. *Nature Communications*, *8*(May), 1–15. <https://doi.org/10.1038/ncomms15423>
- Le Hir, G., Ramstein, G., Donnadieu, Y., & Godd eris, Y. (2008). Scenario for the evolution of atmospheric pCO₂ during a snowball Earth. *Geology*, *36*(1), 47–50. <https://doi.org/10.1130/G24124A.1>
- Lisse, C. M., Wyatt, M. C., Chen, C. H., Morlok, A., Watson, D. M., Manoj, P., et al. (2012). Spitzer evidence for a late-heavy bombardment and the formation of ureilites in η corvi at similar to 1 Gyr. *Astrophysical Journal*, *747*(2), 93. <https://doi.org/10.1088/0004-637X/747/2/93>
- Marchi, S., Bottke, W., Elkins-Tanton, L., Bierhaus, M., Wuennemann, K., Morbidelli, A., & Kring, D. (2014). Widespread mixing and burial of Earth's Hadean crust by asteroid impacts. *Nature*, *511*(7511), 578. <https://doi.org/10.1038/nature13539>
- Mat, W.-K., Xue, H., & Wong, J. T.-F. (2008). The genomics of LUCA. *Frontiers in Bioscience*, *13*, 5605–5613. <https://doi.org/10.2741/3103>
- Menou, K. (2015). Climate stability of habitable earth-like planets. *Earth and Planetary Science Letters*, *429*, 20–24. <https://doi.org/10.1016/j.epsl.2015.07.046>
- Monnard, P.-A., & Szostak, J. W. (2008). Metal-ion catalyzed polymerization in the eutectic phase in water–ice: A possible approach to template-directed RNA polymerization. *Journal of Inorganic Biochemistry*, *102*(5), 1104–1111. <https://doi.org/10.1016/j.jinorgbio.2008.01.026>
- Mulkidjanian, A. Y., Bychkov, A. Y., Dibrova, D. V., Galperin, M. Y., & Koonin, E. V. (2012). Origin of first cells at terrestrial, anoxic geothermal fields. *Proceedings of the National Academy of Sciences*, *109*(14), E821–E830. <https://doi.org/10.1073/pnas.1117774109>
- Neukum, G., Ivanov, B. A., & Hartmann, W. K. (2001). Cratering records in the inner solar system in relation to the lunar reference system. *Space Science Reviews*, *96*(1-4), 55–86. <https://doi.org/10.1023/A:1011989004263>
- Niihara, T., Beard, S. P., Swindle, T. D., Schaffer, L. A., Miyamoto, H., & Kring, D. A. (2019). Evidence for multiple 4.0–3.7 Ga impact events within the Apollo 16 collection. *Meteoritics & Planetary Science*, *54*(4), 675–698. <https://doi.org/10.1111/maps.13237>
- Nisbet, E. G., & Sleep, N. H. (2001). The habitat and nature of early life. *Nature*, *409*(6823), 1083. <https://doi.org/10.1038/35059210>
- Nisbet, E., Zahnle, K., Gerasimov, M. V., Helbert, J., Jaumann, R., Hofmann, B. A., et al. (2007). Creating habitable zones, at all scales, from planets to mud micro-habitats, on Earth and on Mars. In K. E. Fishbaugh, P. Lognonn e, F. Raulin, D. J. Des Marais, & O. Korabev (Eds.), *Geology and habitability of terrestrial planets* pp. 79–121. New York, NY: Springer New York.
- Paradise, A., & Menou, K. (2017oct). GCM simulations of unstable climates in the habitable zone. *The Astrophysical Journal*, *848*(1), 33.
- Pierazzo, E., Hahmann, A. N., & Sloan, L. C. (2003). Chicxulub and climate: Radiative perturbations of impact-produced s-bearing gases. *Astrobiology*, *3*(1), 99–118. <https://doi.org/10.1089/153110703321632453>
- Polat, A., & Frei, R. (2005). The origin of early Archean banded iron formations and of continental crust, Isua, southern West Greenland. *Precambrian Research*, *138*(1), 151–175. <https://doi.org/10.1016/j.precamres.2005.04.003>
- Ritson, D. J., Battilocchio, C., Ley, S. V., & Sutherland, J. D. (2018). Mimicking the surface and prebiotic chemistry of early Earth using flow chemistry. *Nature Communications*, *9*(1), 1821. <https://doi.org/10.1038/s41467-018-04147-2>
- Sagan, C. (1977). Reducing greenhouses and temperature history of Earth and Mars. *Nature*, *269*(5625), 224–226. <https://doi.org/10.1038/269224a0>
- Sagan, C., & Chyba, C. (1997). The early faint Sun paradox: Organic shielding of ultraviolet-labile greenhouse gases. *Science*, *276*(5316), 1217–1221.
- Shields, A. L., Meadows, V. S., Bitz, C. M., Pierrehumbert, R. T., Joshi, M. M., & Robinson, T. D. (2013). The effect of host star spectral energy distribution and ice-albedo feedback on the climate of extrasolar planets. *Astrobiology*, *13*(8), 715–739. <https://doi.org/10.1089/ast.2012.0961>
- Sleep, N. H. (2015). Evolution of the Earth: Plate tectonics through time, (2nd ed.). In G. Schubert (Ed.), *Treatise on geophysics (second edition)* pp. 145–172. Oxford: Elsevier.
- Sleep, N. H. (2016). Asteroid bombardment and the core of Theia as possible sources for the Earth's late veneer component. *Geochemistry, Geophysics, Geosystems*, *17*, 2623–2642. <https://doi.org/10.1002/2016GC006305>
- Sleep, N. H. (2018). Geological and geochemical constraints on the origin and evolution of life. *Astrobiology*, *18*(9), 1199–1219. <https://doi.org/10.1089/ast.2017.1778>

- Sleep, N. H., & Zahnle, K. (2001). Carbon dioxide cycling and implications for climate on ancient Earth. *Journal of Geophysical Research*, 106(E1), 1373–1399. <https://doi.org/10.1029/2000JE001247>
- Sleep, N. H., Zahnle, K. J., Kasting, J. F., & Morowitz, H. J. (1989). Annihilation of ecosystems by large asteroid impacts on the early earth. *Nature*, 342(6246), 139–142. <https://doi.org/10.1038/342139a0>
- Song, H., Jiang, G., Poulton, S. W., Wignall, P. B., Tong, J., Song, H., et al. (2017). The onset of widespread marine red beds and the evolution of ferruginous oceans. *Nature Communications*, 8(1), 399.
- Stüeken, E. E., Anderson, R. E., Bowman, J. S., Brazelton, W. J., Colangelo-Lillis, J., Goldman, A. D., et al. (2013). Did life originate from a global chemical reactor? *Geobiology*, 11(2), 101–126. <https://doi.org/10.1111/gbi.12025>
- Sutherland, J. D. (2016). The origin of life—Out of the blue. *Angewandte Chemie International Edition*, 55(1), 104–121. <https://doi.org/10.1002/anie.201506585>
- Toner, J., & Catling, D. (2019). Alkaline lake settings for concentrated prebiotic cyanide and the origin of life. *Geochimica et Cosmochimica Acta*, 260, 124–132. <https://doi.org/10.1016/j.gca.2019.06.031>
- Toner, J., & Catling, D. (2019). A carbonate-rich lake solution to the phosphate problem of the origin of life. *Proceedings of the National Academy of Sciences*. <https://doi.org/10.1073/pnas.1916109117>
- Tremaine, S., & Dones, L. (1993). On the statistical distribution of massive impactors. *Icarus*, 106(1), 335–341. <https://doi.org/10.1006/icar.1993.1175>
- Turbet, M., Forget, F., Leconte, J., Charnay, B., & Tobie, G. (2017). CO₂ condensation is a serious limit to the deglaciation of Earth-like planets. *Earth and Planetary Science Letters*, 476(1), 11–21. <https://doi.org/10.1016/j.epsl.2017.07.050>
- Valley, J. W., Peck, W. H., King, E. M., & Wilde, S. A. (2002). A cool early Earth. *Geology*, 30(4), 351–354. [https://doi.org/10.1130/0091-7613\(2002\)030h0351:ACEEi2.0.CO;2](https://doi.org/10.1130/0091-7613(2002)030h0351:ACEEi2.0.CO;2)
- Walker, J. C. G., Hays, P. B., & Kasting, J. F. (1981). A negative feedback mechanism for the long-term stabilization of Earth's surface temperature. *Journal of Geophysical Research*, 86(C10), 9776. <https://doi.org/10.1029/JC086iC10p09776>
- Wilde, S. A., Valley, J. W., Peck, W. H., & Graham, C. M. (2001). Evidence from detrital zircons for the existence of continental crust and oceans on the Earth 4.4 Gyr ago. *Nature*, 409(6817), 175–178. <https://doi.org/10.1038/35051550>
- Wordsworth, R., & Pierrehumbert, R. (2013). Hydrogen-nitrogen greenhouse warming in Earth's early atmosphere. *Science*, 339(6115), 64–67. <https://doi.org/10.1126/science.1225759>
- Zahnle, K., & Sleep, N. H. (2002). Carbon dioxide cycling through the mantle and implications for the climate of ancient Earth. *Geological Society, London, Special Publications*, 199(1), 231–257. <https://doi.org/10.1144/GSL.SP.2002.199.01.12>
- Zellner, N. E. (2017). Cataclysm no more: New views on the timing and delivery of lunar impactors. *Origins of Life and Evolution of Biospheres*, 47(3), 261–280. <https://doi.org/10.1007/s11084-017-9536-3>
- Zimmer, K., Zhang, Y., Lu, P., Chen, Y., Zhang, G., Dalkilic, M., & Zhu, C. (2016). SUPCRTBL: A revised and extended thermodynamic dataset and software package of SUPCRT92. *Computers & geosciences*, 90, 97–111. <https://doi.org/10.1016/j.cageo.2016.02.013>

References from The Supporting Information

- Coogan, L. A., & Dosso, S. E. (2015). Alteration of ocean crust provides a strong temperature dependent feedback on the geological carbon cycle and is a primary driver of the Sr-isotopic composition of seawater. *Earth and Planetary Science Letters*, 415, 38–46. <https://doi.org/10.1016/j.epsl.2015.01.027>